International Journal of Scientific Research and Engineering Development-– Volume 8 Issue 4, July-Aug 2025
Available at www.ijsred.com

RESEARCH ARTICLE OPEN ACCESS

Mitigating Voltage Unbalance in Modern Distribution Network with Distributed Energy Resources and Solar PV Inverters

S Surendar
Electrical and Electronics Engineering, Jawaharlal Nehru Technological University Hyderabad
Email: surendar.ai.108@gmail.com

----------**********----------

Abstract:

Maintaining voltage balance in distribution networks is increasingly challenging due to the rise of 1-phase DERs, [15] such as rooftop PV systems, and large 1-phase loads like electric vehicles, which can degrade power quality and reduce equipment efficiency. This study proposes a reactive power compensation strategy using PV inverters, employing two control frameworks: a decentralized controller using only local measurements, and a distributed controller coordinating multiple inverters via communication. Simulations on the IEEE 13-bus feeder under different load and PV conditions show that both controllers effectively improve voltage balance, with the distributed controller achieving superior performance, while the decentralized approach provides a simpler and more economical solution. These results demonstrate that inverter-based reactive power support is a practical and cost-effective method for enhancing voltage stability in high DER penetration networks.

Keywords — **Steinmetz design, Voltage unbalance, Distributed generation, Solar photovoltaic, Decentralized control**

----------**********----------

I. INTRODUCTION

The rapid growth of 1-phase DERs, including rooftop PV systems and EV chargers, has created significant voltage unbalance in distribution networks. [15] This unbalance increases system losses, reduces equipment efficiency, and shortens the lifespan of critical components such as transformers, motors, and protective devices.

Traditional reducing methods, such as network reconfiguration and reactive power devices like SVCs and STATCOMs, are technically effective but costly, complex, and often impractical for conventional feeders without advanced automation. Centralized optimization approaches, while optimal, require heavy computation, extensive communication, and real-time data, limiting their scalability.

To address these challenges, this study introduces a Steinmetz-based reactive power compensation strategy using PV inverters. Two control approaches are considered: a decentralized method, where each inverter operates independently using local measurements, and a distributed method, where inverters coordinate via limited communication to improve overall network performance.

Simulations on the IEEE 13-node feeder under various loading and PV scenarios show that both approaches effectively improve voltage balance. [15] The distributed controller achieves the best performance but requires communication infrastructure, whereas the decentralized method provides a simpler, communication-free, and cost-effective solution.

These results demonstrate that inverter-based reactive power support is a practical and economical means to enhance voltage stability in modern distribution networks with high DER penetration, offering insights for scalable and real-world implementations.

II CONTROL STRATEGIES

Control strategies aimed at reducing voltage unbalance in power distribution systems are essential for maintaining 3-phase voltage symmetry, [15] improving overall power quality, and extending the service life of electrical equipment. Voltage unbalance typically arises from uneven 1-phase loading, asymmetrical distributed generation, or unequal line impedances within the network. Several control approaches have been explored in literature, including Decentralized Control, Distributed Control, Model-Free Control, and Steinmetz-Based Design.

1. Decentralized Controller

In this scheme, each PV inverter operates independently based solely on local measurements, without requiring coordination or communication with other inverters. The controller seeks to simultaneously balance voltages across the 3- phases, thereby indirectly improving the condition at the most critical node. However, complete balance is rarely attainable due to several limitations, such as inverter phase connection constraints, time-varying reactive power capacity, and the simultaneous execution of Steinmetz design at multiple locations. Consequently, each participating PV system applies the same compensation mechanism, which effectively reduces—but does not entirely eliminate—voltage unbalance.

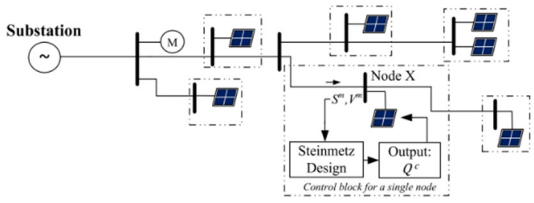

Fig.1.Schematic Diagram of Decentralized Controller

In this scheme, each PV inverter operates independently, [15] relying solely on local voltage and power measurements to determine its reactive power injection Qc.The compensation is regulated within the inverter's capacity limits, and when multiple PV units are connected at the same node, the required Qc is proportionally shared among them. This process is executed periodically to suppress voltage unbalance across the feeder. However, the absence of coordination may result in issues such as **overcompensation or oscillatory responses**. These drawbacks can be alleviated through corrective measures, including restricting the number of active inverters or employing asynchronous update mechanisms.

2.Distributed Controller

In this control framework, photovoltaic inverters operate within a coordinated network of controllers that exchange information through a communication link. [15] Unlike the decentralized approach, which depends solely on local measurements, the distributed controller aims to balance voltages at a designated **critical node** by directing downstream PV systems. At this node, complex voltage and power measurements are processed to compute the required reactive power compensation Qc . The calculated value is then proportionally distributed among the participating inverters, with each device

injecting reactive power within its rated capacity. Since line losses and network dynamics may cause deviations between the delivered and required compensation, the scheme incorporates a feedback loop to iteratively refine inverter outputs. This coordinated strategy achieves superior voltage balancing compared to decentralized control. However, it requires a reliable communication infrastructure, and its performance may be affected by **latency, packet loss, or other communication-related issues**.

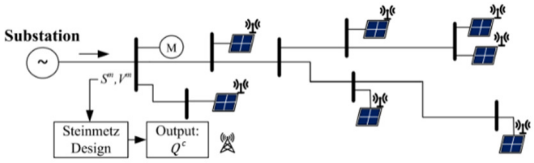

Fig .2 Schematic Diagram of Distributed Controller

In distributed control, V_m and S_m at a critical node are measured to compute the required reactive power compensation Qc, which is then proportionally shared among downstream PV inverters within their capacity limits. A feedback loop ensures iterative refinement for improved accuracy. While this method achieves better voltage unbalance mitigation than decentralized control, its reliance on communication networks makes it vulnerable to delays and data errors.

3.Model-Free Controller

The **MFC** improves voltage balance without requiring detailed network models, relying instead on real-time measurements to guide reactive power adjustments. Its operation is based on phase deviations from the average voltage:

- If a phase voltage is **below** the average, the inverter injects reactive power.
- If a phase voltage is **above** the average, the inverter absorbs reactive power.

Similar to distributed control, MFC functions in a feedback loop using measurements at the critical node. However, by avoiding model dependence, it offers robustness against uncertainties and time-varying feeder conditions.

4. Steinmetz design

The **Steinmetz-based approach** originates from the classical technique of enabling three-phase motors to operate from 1-phase supplies by creating an artificial rotating magnetic field using capacitors. [15] In modern distribution networks with high penetration of 1-phase PV systems and EV chargers, this principle is adapted by utilizing PV inverters to inject reactive power, thereby mitigating voltage unbalance without reducing active power output. Two control modes are commonly employed: **decentralized**, where inverters act independently using local measurements, and **distributed**, where inverters coordinate to share compensation duties. Compared with centralized optimization, Steinmetz-based controllers are simpler, scalable, and practical for real-world applications. Ongoing research addresses challenges such as inverter capacity limits, communication delays, and regulatory considerations for large-scale deployment.

III PROBLEM DESCRIPTION

In a 3-phase system, the $V1$, $V2$, and $V0$ voltages can be obtained using the Fortescue symmetrical component transformation, [15] which decomposes unbalanced phase voltages into their corresponding balanced components.

$$\begin{bmatrix} V_0 \\ V_1 \\ V_2 \end{bmatrix} = \frac{1}{3} \begin{bmatrix} 1 & 1 & 1 \\ 1 & a & a^2 \\ 1 & a^2 & a \end{bmatrix} \begin{bmatrix} V_A \\ V_B \\ V_C \end{bmatrix}, \quad (1)$$

The constant a=ej2π/3=1∠120 and V_A, V_B, V_C represent the phase to neutral voltages of the system. To assess voltage unbalance, **VUFs** are commonly used. The **VUF_2** is defined as the ratio of negative- to positive-sequence voltage, while the zero-sequence unbalance factor is expressed as the ratio of zero- to positive-sequence voltage, usually reported in percentage form. In practice, the main

objectives are to minimize V_2 to reduce zero-sequence unbalance.

Modern distribution feeders are increasingly populated with 1-phase PV systems connected at different nodes. This uneven distribution of generation, combined with unbalanced lines, loads, or regulator tap settings, contributes to voltage unbalance. Such unbalance typically appears as unequal phase magnitudes or phase-angle deviations in the 3-phase voltages.

For large 3-phase equipment, including power transformers and induction motors, voltage unbalance can result in excessive heating, reduced efficiency, and a shorter service life. To avoid equipment damage, it is essential to maintain balanced voltages at critical nodes where such devices are connected.

A practical method to achieve this balance is through **reactive power support from PV inverters**, which can provide compensation without reducing active power generation. Since PV systems generally operate below their rated apparent power capacity, they are capable of supplying reactive support within limits determined by their instantaneous active power output and rated capacity.

$$Q_{i,t}^{\lim} = \pm\sqrt{(S_i^{\text{rate}})^2 - (P_{i,t})^2}, \quad (2)$$

Reactive power regulation, applicable to both PV inverters and EV chargers, is an effective means to mitigate voltage unbalance in distribution systems. While centralized OPF-based optimization offers optimal results, it is computation-intensive and difficult to scale. The **Steinmetz design** provides a practical alternative by relying only on local voltage and power measurements, using linear equations, and requiring minimal communication.

Two control modes are considered. In the **decentralized approach**, each inverter operates independently using local data, contributing reactive power within its limits to improve overall balance. In the **distributed approach**, a central controller at a critical node computes the required compensation and assigns reactive power setpoints to downstream inverters proportionally to their ratings. The decentralized method is simpler and communication-free, while the distributed method achieves better coordination and performance with limited communication.

$$Q_i^c = Q_\phi^c \times \frac{S_i^{\text{rate}}}{\sum_{j\in\Omega_\phi} S_j^{\text{rate}}}, \quad (3)$$

REACTIVE POWER INJECTION USING STEINMETZ DESIGN

For each phase, the required reactive power is denoted as QcϕQ , with Ωϕ representing the set of PV inverters connected to that phase. [15] Each inverter adjusts its reactive power injection as closely as possible to QcϕQ , subject to its capacity limits. Since feeder voltages, losses, and generation levels vary over time, this process operates in a continuous feedback loop where updated measurements are collected, new compensation values are computed, and revised control commands are applied to sustain improved voltage balance.

To evaluate performance, five compensation cases are considered based on network configuration and PV connection type:

- **Case 1:** 3-wire network with delta-connected loads and PVs – only V_2 is mitigated.
- **Case 2:** 4-wire network with delta PVs – mitigation restricted to V_2.
- **Case 3:** 4-wire network with wye PVs – reactive power compensates V_2.
- **Case 4:** 4-wire network with wye PVs – reactive power compensates V_0.
- **Case 5:** Mixed networks with delta and wye PVs – enables mitigation of both V_2 and V_0.

This classification illustrates how the Steinmetz-based control can be adapted to different system topologies, allowing PV inverters to play an active role in enhancing power quality across distribution feeders.

TABLE I CASE SUMMARY

Case	1	2	3	4	5
Load	Δ	Δ & Y	Δ & Y	Δ & Y	Δ & Y
PV	Δ	Δ	Y	Y	Δ & Y
Objective	VUF_2	VUF_2	VUF_2	VUF_0	VUF_2 & VUF_0

Case 1: Delta-Connected Load and Delta-Connected PV (Objective: Mitigate V2V)

In this configuration, both the load and the PV system are delta-connected, as shown in Fig. 2(a). At the critical node, the line-to-neutral voltages VmA,VmB,VmC and corresponding complex powers SmA,SmB,SmC are measured. [15]Using these values, the phase currents are derived by relating each power measurement to its respective voltage. Since the delta-load currents can be expressed with respect to an arbitrary constant that captures unknown load parameters, these relationships serve as the foundation for computing the required reactive power injections within the Steinmetz framework. The control goal in this case is to eliminate the negative-sequence voltage component at the node.

$$\begin{bmatrix} I_{AB}^{tot} \\ I_{BC}^{tot} \\ I_{CA}^{tot} \end{bmatrix} = \begin{bmatrix} I_{AB}^{eq} \\ I_{BC}^{eq} \\ I_{CA}^{eq} \end{bmatrix} + K \begin{bmatrix} 1 \\ 1 \\ 1 \end{bmatrix} = \frac{1}{3} \begin{bmatrix} 1 & -1 & 0 \\ 1 & 2 & 0 \\ -2 & -1 & 0 \end{bmatrix} \begin{bmatrix} I_m^A \\ I_m^B \\ I_m^C \end{bmatrix} + K \begin{bmatrix} 1 \\ 1 \\ 1 \end{bmatrix}. \quad (4)$$

The line-to-line voltages are $V^m{}_{AB}=V^m{}_A-V^m{}_B$, $V^m{}_{BC}=V^m{}_B-V^m{}_C$, $V^m{}_{CA}=V^m{}_C-V^m{}_A$, so the equivalent delta-load demand can be written,

$$S_{AB}^{tot} = V_{AB}^m \left(I_{AB}^{eq} + K\right)^* = S_{AB}^{eq} + V_{AB}^m K^*,$$
$$S_{BC}^{tot} = V_{BC}^m \left(I_{BC}^{eq} + K\right)^* = S_{BC}^{eq} + V_{BC}^m K^*,$$
$$S_{CA}^{tot} = V_{CA}^m \left(I_{CA}^{eq} + K\right)^* = S_{CA}^{eq} + V_{CA}^m K^*.$$

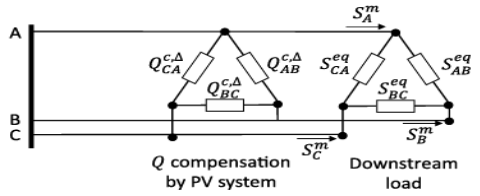

Fig 3 Delta-Connected Load and Delta-Connected PV

Reactive Power Compensation by 3-Phase PV Systems. In this setup, the downstream load is modeled as the equivalent three-phase delta-connected load seen at the critical node, together with additional loads and PV active power injections along the feeder.

- **Case 1 (Delta-connected PV system):** The control objective is to remove the negative-sequence unbalance by forcing the negative-sequence current I_2 to zero, assuming the upstream grid remains balanced.
- This is achieved by tuning the reactive power injections of the delta-connected PV inverter across its 3 branches: Qc,ΔABQ and Qc,ΔCAQ
- After applying these compensations, the resulting delta-load currents are reshaped so that the negative-sequence voltage component V_2 is suppressed at the node.

This approach highlights how delta-connected PV inverters can be leveraged to supply branch-specific reactive power that cancels negative-sequence effects, thereby improving voltage balance in distribution feeders.

$$I_{AB}^{c,tot} = \left(\frac{S_{AB}^{eq} + V_{AB}^m K^* + jQ_{AB}^{c,\Delta}}{V_{AB}^c}\right)^* = I_{AB}^c + K\left(\frac{V_{AB}^m}{V_{AB}^c}\right)^*, \quad (5a)$$
$$I_{BC}^{c,tot} = \left(\frac{S_{BC}^{eq} + V_{BC}^m K^* + jQ_{BC}^{c,\Delta}}{V_{BC}^c}\right)^* = I_{BC}^c + K\left(\frac{V_{BC}^m}{V_{BC}^c}\right)^*, \quad (5b)$$
$$I_{CA}^{c,tot} = \left(\frac{S_{CA}^{eq} + V_{CA}^m K^* + jQ_{CA}^{c,\Delta}}{V_{CA}^c}\right)^* = I_{CA}^c + K\left(\frac{V_{CA}^m}{V_{CA}^c}\right)^*, \quad (5c)$$

Where VcAB,VcBC, denote the compensated line-to-line voltages, the associated sequence currents Ic0,Ic1,Ic2are obtained by applying the Fortescue

symmetrical component transformation in conjunction with Kirchhoff's current law.

$$\begin{bmatrix} I_0^c \\ I_1^c \\ I_2^c \end{bmatrix} = \begin{bmatrix} 1 & 1 & 1 \\ 1 & a^2 & a \\ 1 & a & a^2 \end{bmatrix}^{-1} \begin{bmatrix} 1 & 0 & -1 \\ -1 & 1 & 0 \\ 0 & -1 & 1 \end{bmatrix} \begin{bmatrix} I_{AB}^{c,tot} \\ I_{BC}^{c,tot} \\ I_{CA}^{c,tot} \end{bmatrix}, \quad (6)$$

Solving for I2 in (6) and setting the result to zero yields,

$$\begin{aligned} 3I_2^c &= (1-a^2)I_{AB}^c + (a^2-a)I_{BC}^c + (a-1)I_{CA}^c \\ &\quad + K\left[(1-a^2)\left(\frac{V_{AB}^m}{V_{AB}^c}\right)^* + (a^2-a)\left(\frac{V_{BC}^m}{V_{BC}^c}\right)^* + (a-1)\left(\frac{V_{CA}^m}{V_{CA}^c}\right)^*\right] \quad (7) \\ &= 0. \end{aligned}$$

When the controller balances the line voltages, the compensated values closely match the measured ones, making the term with K negligible—a condition that also holds when the node is fully balanced.

$$V_{BC}^c = a^2 V_{AB}^c, \quad V_{CA}^c = aV_{AB}^c. \quad (8)$$

Using (5) and (8) to simplify (7) and then splitting in to real and imaginary parts gives,

$$Q_{AB}^{c,\Delta} + Q_{BC}^{c,\Delta} - 2Q_{CA}^{c,\Delta} = -\sqrt{3}\,(P_{AB}^{eq} - P_{BC}^{eq}) - (Q_{AB}^{eq} + Q_{BC}^{eq}) + 2Q_{CA}^{eq}, \quad (9a)$$

$$Q_{AB}^{c,\Delta} - Q_{BC}^{c,\Delta} = \frac{1}{\sqrt{3}}\,(P_{AB}^{eq} + P_{BC}^{eq} - 2P_{CA}^{eq}) - (Q_{AB}^{eq} - Q_{BC}^{eq}), \quad (9b)$$

At the critical node, each phase's complex power must satisfy the balancing conditions. [15]However, with three unknown reactive power adjustments in the delta branches and only 2 governing equations, the system is underdetermined, leading to multiple possible solutions. To resolve this, an additional constraint is introduced. Common approaches include enforcing unity power factor, minimizing the quadratic sum of reactive adjustments, or setting the net reactive change to zero. The last option is the most practical, as it preserves the system's overall reactive demand, maintains voltage stability, and minimizes feeder disturbances.

$$Q_{AB} \cdot \Delta + Q_{BC} \cdot \Delta + Q_{CA} \cdot \Delta = 0. \quad ($$

Is preferable. Combining (9) and (10) gives the final 3-phase reactive power compensation strategy,

$$Q_{AB}^{c,\Delta} = \frac{1}{3}\left(Q_{CA}^{eq} + Q_{BC}^{eq} - 2Q_{AB}^{eq} + \sqrt{3}(P_{BC}^{eq} - P_{CA}^{eq})\right), \quad (11a)$$

$$Q_{BC}^{c,\Delta} = \frac{1}{3}\left(Q_{AB}^{eq} + Q_{CA}^{eq} - 2Q_{BC}^{eq} + \sqrt{3}(P_{CA}^{eq} - P_{AB}^{eq})\right), \quad (11b)$$

$$Q_{CA}^{c,\Delta} = \frac{1}{3}\left(Q_{BC}^{eq} + Q_{AB}^{eq} - 2Q_{CA}^{eq} + \sqrt{3}(P_{AB}^{eq} - P_{BC}^{eq})\right), \quad (11c)$$

Case 2: Delta and Wye Load with Delta-Connected PV (Target: Eliminate V_2)

Wye loads are converted into an equivalent delta form, introducing an additional zero-sequence current. [15]The Steinmetz method is then applied to the equivalent delta currents, allowing the delta-connected PV inverter to mitigate the negative-sequence voltage component. elimination of the negative-sequence voltage V_2.

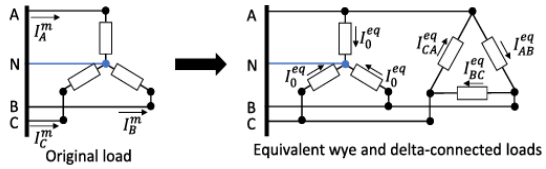

Fig 4 Delta and Wye Load, Delta PV

Case 3: Wye PV, Eliminate V2

For wye-connected PV systems, the compensated line currents are obtained by adding the inverter's reactive injections to the original currents. Using the Fortescue transformation, [15]the negative-sequence component is set to zero, giving two conditions that link the three phase injections. Since this leaves one degree of freedom, an extra constraint is applied to determine a unique solution within inverter limits.

$$3I_2^c = I_A^c + a^2 I_B^c + aI_C^c = 0$$

Where

$$I_A^c = \left(\frac{S_A^m + jQ_A^{c,Y}}{V_A^c}\right)^*, \quad (13a)$$

$$I_B^c = \left(\frac{S_B^m + jQ_B^{c,Y}}{V_B^c}\right)^*, \quad (13b)$$

$$I_C^c = \left(\frac{S_C^m + jQ_C^{c,Y}}{V_C^c}\right)^*. \quad (13c)$$

Eliminating the negative-sequence component V_2 ensures balance among the line-to-line voltages, but

it does not automatically guarantee balance in the line-to-neutral voltages since the zero-sequence component V_0 may still exist. However, for analysis, we assume that the line-to-neutral voltages remain balanced.

$$V_B^c = a^2 V_A^c, \quad V_C^c = a V_A^c. \tag{14}$$

By enforcing that the total change in reactive power injections equals zero, a practical compensation strategy is derived for balancing the system.

$$Q_A^{c,Y} = \frac{1}{3}\left(Q_C^m + Q_B^m - 2Q_A^m + \sqrt{3}(P_B^m - P_C^m)\right), \tag{15a}$$
$$Q_B^{c,Y} = \frac{1}{3}\left(Q_A^m + Q_C^m - 2Q_B^m + \sqrt{3}(P_C^m - P_A^m)\right), \tag{15b}$$
$$Q_C^{c,Y} = \frac{1}{3}\left(Q_B^m + Q_A^m - 2Q_C^m + \sqrt{3}(P_A^m - P_B^m)\right), \tag{15c}$$

If the zero-sequence voltage V_0 is significant, the earlier approximation may not hold. In such cases, it is more appropriate to estimate the compensated line-to-neutral voltages using the actual measured values.

$$V_A^c = V_A^m, \quad V_B^c = V_B^m, \quad V_C^c = V_C^m. \tag{16}$$

Then, the three-phase reactive power compensation strategy is given by the solution of,

$$\mathrm{Re}\{I_2^c\} = \mathrm{Im}\{I_2^c\} = 0, \tag{17a}$$
$$Q_A^{c,Y} + Q_B^{c,Y} + Q_C^{c,Y} = 0. \tag{17b}$$

Due to the approximations used, the reactive power adjustments cannot fully remove V_2. However, through the feedback process,V_2 typically converges to a value very close to zero.

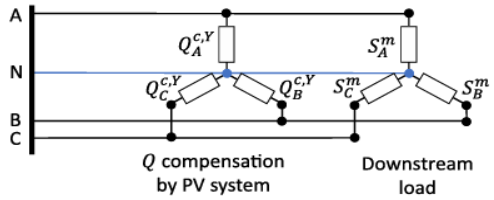

Fig 5 Wye PV Eliminate V2 & V0

Cases 3 and 4: Wye-connected PV system used to eliminate negative- or zero-sequence unbalance.

Case 4: Wye PV, Eliminate V_0

It assumes the same connections as Case 3 but drives the zero-sequence current to zero,

$$3I_0^c = I_A^c + I_B^c + I_C^c = 0. \tag{18}$$

Let assume the voltages are balanced (14), then the reactive power compensation strategy is given by,

$$Q_A^{c,Y} = \frac{1}{3}\left(Q_C^m + Q_B^m - 2Q_A^m + \sqrt{3}(P_C^m - P_B^m)\right), \tag{19a}$$
$$Q_B^{c,Y} = \frac{1}{3}\left(Q_A^m + Q_C^m - 2Q_B^m + \sqrt{3}(P_A^m - P_C^m)\right), \tag{19b}$$
$$Q_C^{c,Y} = \frac{1}{3}\left(Q_B^m + Q_A^m - 2Q_C^m + \sqrt{3}(P_B^m - P_A^m)\right), \tag{19c}$$

Suppressing V_0 can sometimes worsen V_2, leading to unbalanced line-to-line and line-to-neutral voltages. [15]As an alternative, the voltages can be approximated by their measured values, similar to the approach in (16). In this case, the compensation method retains the same structure as (17), but with the condition in (17a) replaced accordingly.

$$\mathrm{Re}\{I_0^c\} = \mathrm{Im}\{I_0^c\} = 0. \tag{20}$$

Because of the voltage approximation, feedback is again used to drive V_0 close to zero.

Case 5: Delta and Wye PV (Eliminating V_2 and V_0)

In this setup, delta- and wye-connected PV systems operate together to correct both negative- and zero-sequence unbalances. [15] This ensures balance in both line-to-line and line-to-neutral voltages. The strategy drives the I_2- and I_0 to zero while keeping the total reactive power injection from all PV units equal to zero. Solving under these constraints yields the required compensation plan, allowing coordinated mitigation of both unbalance components.

$$Q_A^{c,Y} = \frac{1}{3}\left(Q_C^m + Q_B^m - 2Q_A^m + \sqrt{3}(P_C^m - P_B^m)\right), \quad (21a)$$

$$Q_B^{c,Y} = \frac{1}{3}\left(Q_A^m + Q_C^m - 2Q_B^m + \sqrt{3}(P_A^m - P_C^m)\right), \quad (21b)$$

$$Q_C^{c,Y} = \frac{1}{3}\left(Q_B^m + Q_A^m - 2Q_C^m + \sqrt{3}(P_B^m - P_A^m)\right), \quad (21c)$$

$$Q_{AB}^{c,\Delta} = \frac{2}{\sqrt{3}}(P_B^m - P_A^m), \quad (21d)$$

$$Q_{BC}^{c,\Delta} = \frac{2}{\sqrt{3}}(P_C^m - P_B^m), \quad (21e)$$

$$Q_{CA}^{c,\Delta} = \frac{2}{\sqrt{3}}(P_A^m - P_C^m), \quad (21f)$$

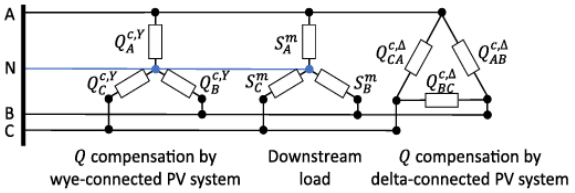

Fig 7 Delta and Wye PV

Flowchart of Voltage Unbalance Mitigation Using Reactive Power Injection

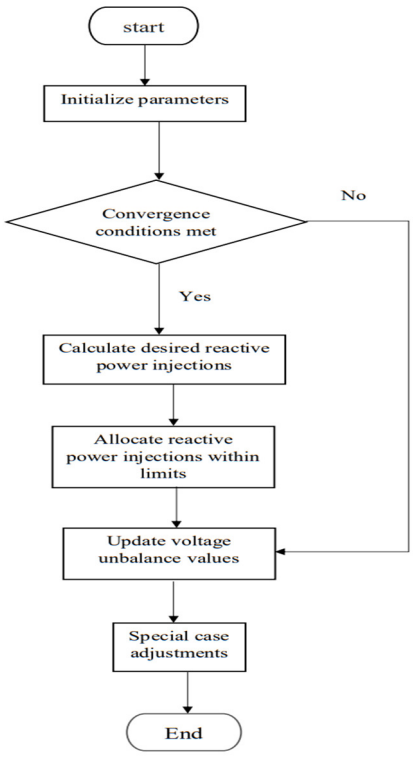

CASE STUDY

The IEEE 13-node feeder, a benchmark model developed by the IEEE Power & Energy Society, is widely used for testing distribution system analysis and control methods. [15]As a 4-wire network with both delta- and wye-connected loads, it provides a suitable platform for examining Cases 2–5. The feeder setup is first described in detail, after which it is applied to evaluate and compare the performance of the proposed controllers.

TABLE II
SINGLE-PHASE PV SYSTEMS ADDED TO 13-NODE FEEDER

#	1	2	3	4	5	6	7	8	9	10	11
Location	632	633	634	645	646	671	652	611	680	692	675
Phase	2	1	1	2	2	1	3	3	2	3	1
P (kW)	100	150	60	100	100	50	100	50	50	100	110

IEEE 13-Node Feeder Setup

The study uses the IEEE 13-node feeder, with complete data for nodes and lines. [15] The feeder comprises constant impedance, current, and power loads. To highlight voltage unbalance, all loads are uniformly increased by 10%, and Node 632 is selected as the critical point for analysis

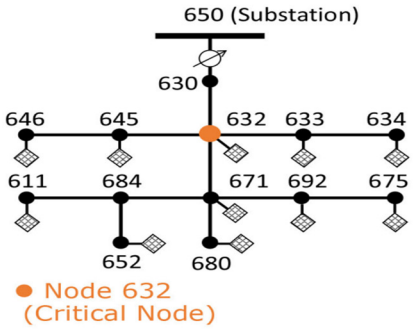

Fig 8 IEEE 13-node feeder

The feeder was modified by setting all regulator taps to position 11 and transposing the feeder lines to reduce upstream unbalance. [15]Selected lines were reconfigured as three-phase to allow PV integration. A total of 11 single-phase PV units (300 kVA each) were installed, with a mix of line-to-line and line-to-neutral connections depending on the case. PVs at non–three-phase nodes were excluded from control. Altogether, the PVs supplied 970 kW, about 25% of the total feeder load of 3813 kW.

IV. RESULTS AND ANALYSIS

Matlab Code Results

Zero sequence unbalance factor VS Iteration

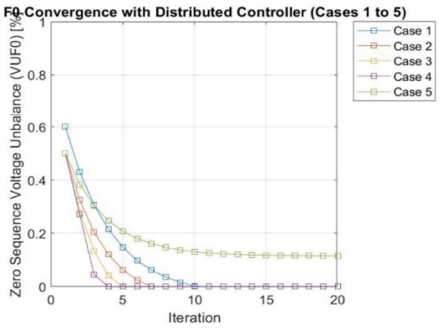

Fig 9 Zero sequence unbalance factor VS Iteration

The results show that distributed controllers significantly reduce V_0 unbalance. With increasing iterations, VUF_0 steadily decreases, with Case 4 demonstrating the fastest and most complete mitigation.

Negative sequence unbalance factor VS Iteration

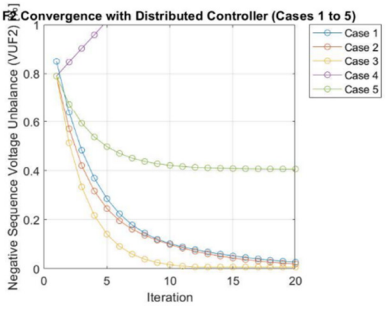

Fig 10 Negative sequence unbalance factor VS Iteration

The graph indicates that the distributed controller effectively mitigates VUF_2 in most cases as iterations progress. Case 3 shows the fastest convergence, whereas Case 4 deteriorates over time, highlighting controller limitations.

Total reactive power injection (KVAR) VS Iteration

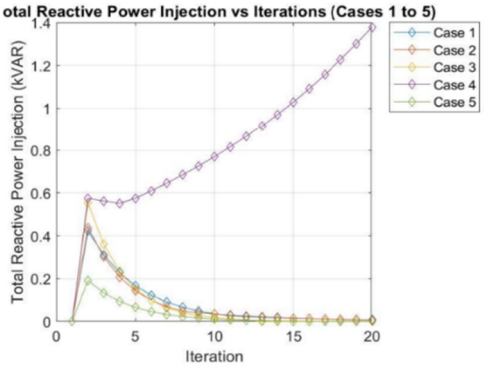

Fig 11 Total reactive power injection (KVAR) VS Iteration

As iterations progress, reactive power injection decreases in Cases 1, 2, 3, and 5, showing effective controller convergence with minimal steady-state demand. In contrast, Case 4 exhibits continuously rising reactive power injection, indicating instability and poor control. This highlights how controller design and PV configuration strongly affect both convergence behaviour and reactive power requirements.

Reactive power injection (p.u) VS Iteration

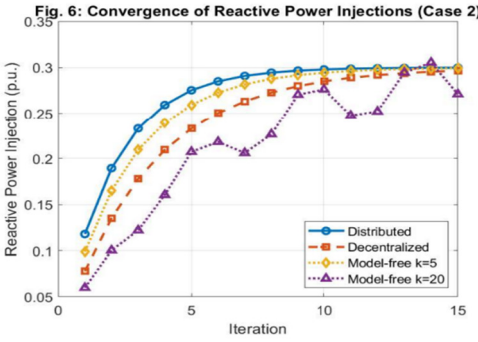

Fig 12 Reactive power injection (p.u) VS Iteration

The graph compares control strategies for reactive power injection over iterations. [15] The Distributed controller achieves the fastest and most stable convergence (0.3p.u.), followed by the Decentralized method. Model-free controllers with k=5 and k=20 converge more slowly and show

fluctuations, with k=5k performing better. These results demonstrate the superior stability and speed of distributed control for reactive power regulation.

VUF2 at critical node (%) VS Iteration

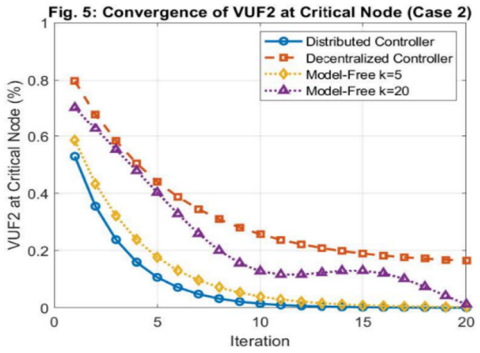

Fig 13 VUF2 at critical node (%) VS Iteration

The plot illustrates the reduction of VUF_2 over 20 iterations using four control methods.The Distributed Controller achieves the fastest and most effective reduction, nearly eliminating unbalance. [15] The Decentralized Controller performs slower and less efficiently, while Model-Free controllers reduce VUF_2 more gradually, with k=5 outperforming k=20. Overall, distributed control provides the best performance in minimizing voltage unbalance.

VUF2 (%) VS Iteration

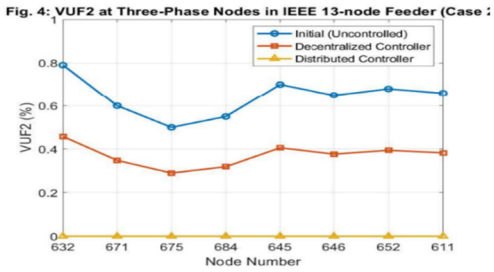

Fig 13 VUF2 (%) VS Iteration

The figure compares VUF_2 across several nodes under three conditions: Initial (Uncontrolled), Decentralized Controller, and Distributed Controller. In the Initial case, VUF_2 is relatively high (0.5%–0.8%). The Decentralized Controller reduces it to about 0.3%–0.5%, while the Distributed Controller achieves near-zero unbalance across all nodes, demonstrating superior performance in minimizing voltage unbalance throughout the feeder.

COMPARISION

IEEE 13-node feeder

Node Number	VUF (%) Initial (Uncontrolled)	VUF (%) Decentralized Controller	VUF (%) Distributed Controller
632	0.80	0.47	0.01
671	0.65	0.40	0.01
675	0.55	0.30	0.01
684	0.58	0.33	0.01
645	0.70	0.43	0.01
646	0.66	0.39	0.01
652	0.68	0.41	0.01
611	0.65	0.39	0.01

V. CONCLUSION AND FUTURE WORK

The study demonstrates that distributed controllers outperform decentralized ones in reducing voltage unbalance, [15]thanks to coordinated reactive power control from PV systems. Performance depends on controller placement, with upstream deployment improving results for distant critical nodes, though distributed control requires communication infrastructure.

Future research will compare decentralized and distributed controllers with centralized methods, study convergence and robustness under delays or measurement errors, and explore incentives for PV owners to provide reactive power support for unbalance mitigation.

REFERENCES

[1] X. Su, M.A. Masoum, and P.J. Wolfs, "Optimal PV inverter reactive power control and real power curtailment to improve performance of unbalanced four-wire LV distribution networks," IEEE Trans. Sustain. Energy, vol.5, no. 3, pp. 967–977, Jul. 2014.

[2] O. Jordi, L. Sainz, and M. Chindris, "Steinmetz system design under un balanced conditions," Eur. Trans. Elect. Power, vol. 12, no.4, pp. 283–290, 2002.

[3] L. Monjo, L. Sainz, S. Riera, and J. Bergas, "Theoretical study of the Steinmetz circuit design," Electric Power Compon. Syst., vol. 41, no. 3, pp. 304–323, 2013.
[4] M. Yao, I. A. Hiskens and J. L. Mathieu, "Applying Steinmetz circuit design to mitigate voltage unbalance using distributed solar PV," in IEEE Power Tech, 2019, pp. 1–6.
[5] A. Von Jouanne and B. Banerjee, "Assessment of voltage unbalance," IEEE Trans. Power Del., vol. 16, no. 4, pp. 782–790, Oct. 2001.
[6] S.-Y. Lee and C.-J. Wu, "On-line reactive power compensation schemes for unbalanced three phase four wire distribution feeders," IEEE Trans. Power Del., vol. 8, no. 4, pp. 1958–1965, Oct. 1993.
[7] R.P. Broadwater, A. H. Khan, H. E. Shaalan, and R.E. Lee, "Time varying load analysis to reduce distribution losses through reconfiguration," IEEE Trans. Power Del., vol. 8, no. 1, pp. 294–300, Jan. 1993.
[8] F. Shahnia, P.J. Wolfs, and A. Ghosh, "Voltage unbalance reduction in low voltage feeders by dynamic switching of residential customers among three phases," IEEE Trans. Smart Grid, vol. 5, no. 3, pp. 1318–1327, May2014.
[9] R. Otto, T. Putman, and L. Gyugyi, "Principles and applications of static, thyristor-controlled shunt compensators," IEEE Trans. Power App. Syst., vol. PAS-97, no. 5, pp. 1935–1945, Sep. 1978.
[10] J.-H. Chen, W.-J. Lee, and M.-S. Chen, "Using a static VAR compensator to balance a distribution system," in Proc. IEEE Ind. Appl. Conf., 1996, vol. 4, pp. 2321–2326.
[11] S. Kadam and B. Bletterie, "Balancing the grid with single-phase PV installations," in Proc. IEEE Symp. Ind. Electron., 2017, pp. 63–69.
[12] M. Coppo, A. Raciti, R. Caldon, and R. Turri, "Exploiting inverter interfaced DG for voltage unbalance mitigation and ancillary services in distribution systems," in IEEE Forum Res. Technol. Soc. Ind., 2015, pp. 371–376.
[13] T. Hong and F. De Leon, "Controlling non-synchronous microgrids for load balancing of radial distribution systems," IEEE Trans. Smart Grid, vol. 8, no. 6, pp. 2608–2616, Nov. 2016.
[14]] O. Jordi, L. Sainz, and M. Chindris, "Steinmetz system design under un balanced conditions," Eur. Trans. Elect. Power, vol. 12, no.4, pp. 283–290, 2002.
[15] S. Surendar, "Mitigating voltage unbalance in modern distribution networks," B.Tech thesis, Dept. of Electrical Engineering, JNTUH UCESTH, Hyderabad, India, 2025.

